Alexandria Engineering Journal (2015) **54**, 147–154

HOSTED BY

ELSEVIER

Alexandria University

Alexandria Engineering Journal

www.elsevier.com/locate/aej
www.sciencedirect.com

REVIEW

Similitude and scaling of large structural elements: Case study

CrossMark

M. Shehadeh [a,*], Y. Shennawy [a], H. El-Gamal [b]

[a] *Arab Academy for Science, Technology and Maritime Transport, Alexandria, Egypt*
[b] *Alexandria University, Alexandria, Egypt*

Received 8 April 2014; revised 26 November 2014; accepted 17 January 2015
Available online 14 February 2015

KEYWORDS

Similitude;
Scaling;
Buckingham theorem;
Stress;
Deformation

Abstract Scaled down models are widely used for experimental investigations of large structures due to the limitation in the capacities of testing facilities along with the expenses of the experimentation. The modeling accuracy depends upon the model material properties, fabrication accuracy and loading techniques. In the present work the Buckingham π theorem is used to develop the relations (i.e. geometry, loading and properties) between the model and a large structural element as that is present in the huge existing petroleum oil drilling rigs. The model is to be designed, loaded and treated according to a set of similitude requirements that relate the model to the large structural element. Three independent scale factors which represent three fundamental dimensions, namely mass, length and time need to be selected for designing the scaled down model. Numerical prediction of the stress distribution within the model and its elastic deformation under steady loading is to be made. The results are compared with those obtained from the full scale structure numerical computations. The effect of scaled down model size and material on the accuracy of the modeling technique is thoroughly examined.

Contents

1. Introduction 148
2. Theories of scale model similitude. 148
   2.1. Scaling laws and parameters optimization methods 148
   2.2. Dimensional analysis methods 149
3. Case study 149
   3.1. The pad-eye 149
   3.2. Applying Buckingham π theorem on the pad-eye. 149
   3.3. Case study of prototype pad-eye of a derrick 150

* Corresponding author.
E-mail address: ezzfahmy@aast.edu (M. Shehadeh).
Peer review under responsibility of Faculty of Engineering, Alexandria University.

http://dx.doi.org/10.1016/j.aej.2015.01.005
1110-0168 © 2015 Faculty of Engineering, Alexandria University. Production and hosting by Elsevier B.V.

4. Results and discussion . . . 151
4.1. Deriving the equations factors for the prototype . . . 151
4.2. Mesh information . . . 151
4.3. Deriving the equations factors . . . 151
4.4. Models scaling tests . . . 152
4.5. Discussion . . . 152
5. Conclusions . . . 153
References . . . 153

1. Introduction

Any new design is subjected to many investigations through theoretical analyses and experimental verification. As a system becomes more complex, assumptions are usually made in order to formulate a mathematical model for the system. In the absence of a complete design base, a new system requires extensive experimental evaluation until it gains the necessary reliability and desired performance. For large and "oversize" systems, such as offshore/onshore rigs, tall buildings, dams, bridges, spacecraft, airplanes, and space stations, creating the actual working conditions for testing the prototype most of the time is impossible, as in providing a zero gravitational acceleration condition on the ground for testing large space stations or antennas [8,16,4].

Even when a prototype test is possible, it is expensive, time consuming, and difficult to control. Thus, it is extremely useful if a prototype can be replaced by a similar scale model which is much easier to work with. The only possible way to obtain experimental data of overall performance of such a system and the interaction of its elements is to design a small similar system (scale *model*) which replicates the behavior of the actual system (prototype). The accuracy of the behavior of the prototype, which is predicted from interpreting the test results of the model, is dependent on the relationship between the corresponding variables and parameters of model and its prototype [3].

Similarity of systems requires that the relevant system parameters are identical and these systems are governed by unique set of characteristic equations. Thus, if a relation or equation of variables is written for a system, it is valid for all systems which are similar to it [16,7]. Each variable in a model is proportional to the corresponding variable of the prototype. In establishing similarity conditions between the model and prototype two procedures can be used. The similarity conditions can be established either directly from the field equations of the system or, if it is a new phenomenon and the mathematical model of the system is not available, through dimensional analysis. In the second case, all of the variables and parameters which affect the behavior of the system must be known. By using dimensional analysis, an incomplete form of the characteristic equation of the system can be formulated [4]. This equation is in terms of non-dimensional products of variables and parameters of the system. Then, similarity conditions can be established on the basis of this equation.

2. Theories of scale model similitude

Similitude theory is concerned with establishing necessary and sufficient conditions of similarity between two phenomena. Establishing similarity between systems helps to predict the behavior of a system from the results of investigating other systems which have already been investigated or can be investigated more easily than the original system. The behavior of a physical system depends on many parameters, i.e. geometry, material behavior, dynamic response, and energy characteristic of the system. The nature of any system can be modeled mathematically in terms of its variables and parameters [15].

A prototype and its scale model are two different systems with different parameters. The necessary and sufficient conditions of similitude between prototype and its scale model require that the mathematical model of the scale model can be transformed to that of the prototype by a bi-unique mapping or vice versa [14]. Qian et al. [10] studied the scaling laws for impact damage in fiber composites by experiments. Their experiments on scale plates, made of carbon and subjected to impact loads, were carried out and the scaling laws for scaling (up) the strain responses of the specimens to those of the full-size ones were derived. The results show that the derived scaling laws could reasonably predict the responses of the undamaged carbon plates undergoing impact loads. Simitses et al. [13] studied the design of scale-down models for predicting the laminated shell buckling and free vibration. In their article, the similitude theory is employed to establish the similarity between the chosen structural systems, and then the scaling laws are derived and used to predict the physical characteristics of the full-size structures. Vassalos [17] investigated the physical modeling and similitude of marine structures and provided some valuable information concerning the appropriate use of models in the design of marine structures. Safoniuk et al. [11] presented a method to scale up the three-phase fluidized beds, in which the scaling laws are obtained by achieving geometric and dynamic similitude with the aid of the Buckingham π theorem. Chouchaoui et al. [2] used the similitude theory to develop the scaling laws for predicting the elastic behavior of a laminated cylindrical tube under tension, torsion, bending, internal and external pressure from the corresponding ones of the scale model.

2.1. Scaling laws and parameters optimization methods

Several techniques were introduced where most of the literature uses a gradient-based optimization method and the solution often oscillates or diverges, depending upon the initial search point, since the model and the measurement errors can make the objective function complex [1,5]. One of the approaches used to overcome this problem is to use a robust optimization method and genetic algorithms (GAs) which were successfully used to find the parameter set in a stable manner. Nevertheless, this stability of convergence is achieved only at the expense of efficiency. Taking the advantage of the efficiency of the gradient-based optimization method and the robustness of GAs, this work first proposes a hybrid optimization method, namely gradient-incorporated continuous evolutionary algorithms (GICEAs), which can solve this class of problems efficiently and in a robust manner. This method is an extension of continuous evolutionary algorithms (CEAs). The search point representation of which is continuous unlike GAs, and has demonstrated their capability to yield good approximate solutions one order faster than GAs for complex optimization with a continuous search space. By incorporating gradient search, GICEAs can further accelerate the speed of convergence without sacrificing robustness. The use of this technique, however, still leaves the user to develop algorithms to derive a computer model response for each model and each set of experimental data.

2.2. Dimensional analysis methods

The research efforts moved onto two different streams, one concentrating on the integration of dimensional analysis with other research methodologies, and the other trying to export the use of DA into new research areas different from traditional physics and engineering ones. In the first stream the works of Vignaux and Scott [18], and Mendez and Ordonez [9] on regression and data modeling can be quoted. Regarding the second stream there is the work of Hertkorn and Rudolph [6].

3. Case study

3.1. The pad-eye

A pad-eye is a device often found on boats that a line runs through, or provides an attachment point. It is a kind of fairlead and often bolted or welded to the deck or hull of a boat. It is also used in oil and gas projects to assist in the purpose of lifting. Lifting is done with the help of D-shackle or sling, which fits into the hole of pad-eye. There may be one or more circular plates (cheek plates) welded around the hole. The pad-eye is one of the main and most critical structural elements in derrick structures as it is used at the main connection and lifting points.

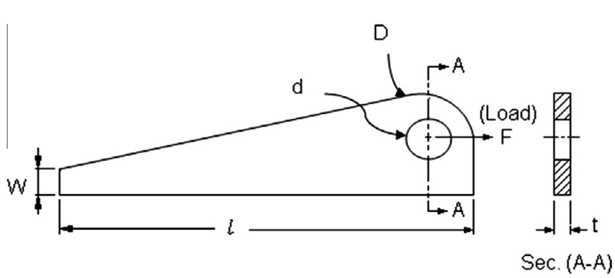

Figure 1 Pad-eye main dimensions.

3.2. Applying Buckingham π theorem on the pad-eye

The aim of this study was to determine a set of dimensionless groups that can be used to correlate data for relating the pad-eye strain due to a static biaxial loading, pad-eye thickness, mating face length, hole diameter, pad-eye outer diameter, pad-eye wedge height and the modulus of elasticity as the main mechanical property which identify the pad-eye material, Fig. 1.

Step 1: List of all parameters involved in the case study.

σ: stress. E: modulus of elasticity.
F: applied force. ρ: Density. W: wedge height. δ: maximum displacement.
I: second moment of area for section A-A. d: hole diameter.
t: pad-eye thickness. D: pad-eye outer diameter. L: Mating face length.

Note: all the expected parameters which are relevant to the problem are included. If this suspicion is correct, experiments will show that the parameter must be included to get consistent result; if the parameter is extraneous, an extra π-group may result but experiments will show that it may be eliminated from consideration. Fig. 1 shows all parameters used in the case study.

Step 2: Identifying the number of restrictions (r).

The number of dimensions depends upon the problem being analyzed. The temperature or the electric or magnetic charges are not to be included.

Primary dimensions selected were (M, L, T). Representing the mass, length and time.
The number of restrictions is equal to the number of primary dimensions.

In this problem (kg, m, s) are selected $r = 3$.

Step 3: Assigning the primary dimensions to the parameters.

The primary conditions of the case study as from Table 1 are

No. of parameters, $n = 11$, No. of restrictions, $r = 3$, No. of π-groups, $k = n - r$.

Thus, $k = 11–3 = 8$ π-groups.

Step 4: Selecting from the parameters the repeating parameters which include all of the primary dimensions.

The following rules are to be considered:

1. Not to pick as repeating parameter that is needed to be isolated. In this case the strain σE.
2. All of the dimensions must be presented in the repeating parameters.

Table 1 System parameters Primary Dimensions.

Parameter	E	F	ρ	t	σ	I	l	D	d	W	δ
Primary dimensions	$ML^{-1}T^{-2}$	MLT^{-2}	ML^{-3}	L	$ML^{-1}T^{-2}$	L^4	L	L	L	L	L

3. A repeating parameter which has the same unit as another repeating parameter to a power is not to be selected.

According to the above rules t, ρ and E have been selected.

Step 5: Deriving the π-groups using the parameters. Repeating parameters and one additional parameter in the format:

Non-repeating variable (σ)

$\pi_1 = \sigma \quad (t^a \cdot \rho^b \cdot E^c) = (ML^{-1}T^{-2}). \quad ((L)^a \cdot (ML^{-3})^b \cdot (ML^{-1}T^{-2})^c)$

$\pi_1 = (kg^1\ m^{-1}\ s^{-2}) \cdot ((m)^a \cdot (kg\ m^{-3})^b \cdot (kg\ m^{-1}\ s^{-2})^c) = (kg)^0 \cdot (m)^0 \cdot (s)^0$

Select values for the powers a, b & c such that dimensions are all to the zero power; (i.e. dimensionless).

$$\left.\begin{array}{l} L: -1 + a - 3b - c = 0 \\ M: 1 + b + c = 0 \\ T: \ -2 - 2c = 0 \end{array}\right\} \begin{array}{l} c = -1 \\ b = 0 \\ a = 0 \end{array}$$

$\pi_1 = \sigma/E$

Non-repeating variable (I)

$\pi_2 = I\ (t^a \cdot \rho^b \cdot E^c) = (L)^4.\ ((L)^a \cdot (ML^{-3})^b \cdot (ML^{-1}T^{-2})^c)$

$\pi_2 = (m)^4 \cdot ((m)^a \cdot (kg\ m^{-3})^b \cdot (kg\ m^{-1}\ s^{-2})^c) = (kg)^0 \cdot (m)^0 \cdot (s)^0$

$$\left.\begin{array}{l} L: 4 + a - 3b + c = 0 \\ M: \ b - c = 0 \\ T: \ -2c = 0 \end{array}\right\} \begin{array}{l} b = 0 \\ c = 0 \\ a = -4 \end{array}$$

$\pi_2 = I/t^4$

Non-repeating variable (L)

$\pi_3 = L\ (t^a \cdot \rho^b.\ E^c) = (L).\ ((L)^a.\ (ML^{-3})^b.\ (ML^{-1}T^{-2})^c)$

$\pi_3 = (m) \cdot ((m)^a \cdot (kg\ m^{-3})^b \cdot (kg\ m^{-1}\ s^{-2})^c) = (kg)^0 \cdot (m)^0 \cdot (s)^0$

$$\left.\begin{array}{l} L: 1 + a - b + c = 0 \\ M: \ b - c = 0 \\ T: \ -2c = 0 \end{array}\right\} \begin{array}{l} b = 0 \\ c = 0 \\ a = -1 \end{array}$$

$\pi_3 = L/t$

Non-repeating variable (d)

$\pi_4 = d\ (t^a \cdot \rho^b \cdot E^c) = (L) \cdot ((L)^a \cdot (ML^{-3})^b \cdot (ML^{-1}T^{-2})^c)$

$\pi_4 = (m) \cdot ((m)^a \cdot (kg\ m^{-3})^b \cdot (kg\ m^{-1}\ s^{-2})^c) = (kg)^0 \cdot (m)^0 \cdot (s)^0$

$$\left.\begin{array}{l} L: 1 + a - b + c = 0 \\ M: \ b - c = 0 \\ T: \ -2c = 0 \end{array}\right\} \begin{array}{l} b = 0 \\ c = 0 \\ a = -1 \end{array}$$

$\pi_4 = d/t$

Non-repeating variable (D)

$\pi_5 = D\ (t^a \cdot \rho^b \cdot E^c) = (L) \cdot ((L)^a \cdot (ML^{-3})^b \cdot (ML^{-1}T^{-2})^c)$

$\pi_5 = (m) \cdot ((m)^a \cdot (kg\ m^{-3})^b \cdot (kg\ m^{-1}\ s^{-2})^c) = (kg)^0 \cdot (m)^0 \cdot (s)^0$

$$\left.\begin{array}{l} L: 1 + a - b + c = 0 \\ M: \ b + c = 0 \\ T \ -2c = 0 \end{array}\right\} \begin{array}{l} b = 0 \\ c = 0 \\ a = -1 \end{array}$$

$\pi_5 = D/t$. Because of the repetition of the same dimension in the π-groups we have $\pi_6 = W/t$, $\pi_7 = \delta/t$.

Non-repeating variable (F)

$\pi_8 = F$

$(t^a \cdot \rho^b \cdot E^c) = (MLT^{-2}) \cdot ((L)^a \cdot (ML^{-3})^b \cdot (ML^{-1}T^{-2})^c)$

$\pi_8 = (kg\ m\ s^{-2}) \cdot ((m)^a \cdot (kg\ m^{-3})^b \cdot (kg\ m^{-1}\ s^{-2})^c) = (kg)^0 \cdot (m)^0 \cdot (s)^0$

$$\left.\begin{array}{l} L: 1 + a - 3b - c = 0 \\ M: \ 1 + b + c = 0 \\ T: \ -2 - 2c = 0 \end{array}\right\} \begin{array}{l} c = -1 \\ b = 0 \\ a = -2 \end{array}$$

$\pi_8 = F/t^2E$. Table 2 shows all the π's relationships.

Step 6: Verifying the dimensionless of the π-groups.

The functional dependence between the π-groups is determined experimentally.

$$\pi_1 = f(\pi_2, \pi_3, \pi_4, \pi_5, \pi_6, \pi_7, \pi_8), \quad \frac{\sigma}{E} = f\left(\frac{l}{t^4}, \frac{L}{t}, \frac{d}{t}, \frac{D}{t}, \frac{W}{t}, \frac{\delta}{t}, \frac{F}{t^2E}\right)$$

Hence the main parameters which required to be grouped are d/D, t, δ, F and σ. The approach is to figure out the equation constant which controls the relationship between those parameters.

To specify the equation constant all parameters have been fixed for the same prototype to check which will be the constant parameter after altering the values of F as well as calculating σ's. The relation which will be used:

$$\pi_1 = S \cdot \frac{\pi_5 \pi_8}{\pi_4} \quad (1)$$

$$\sigma = S \cdot \frac{F \cdot D}{t^2 \cdot d} \quad (2)$$

By applying the same sequence to derive a relation between f and δ

$$\pi_7 = K \cdot \frac{\pi_5 \pi_8}{\pi_4} \quad (3)$$

$$\delta = K \frac{F \cdot D}{E \cdot t \cdot d} \quad (4)$$

where S and K are the σ to F and the δ to F factors respectively.

3.3. Case study of prototype pad-eye of a derrick

As a case study the dimensions of the pad-eye of the derrick raising system and the mean wiring scheme are considered.

Table 2 π's relationships.

π_1	π_2	π_3	π_4	π_5	π_6	π_7	π_8
$\frac{\sigma}{E}$	$\frac{l}{t^4}$	$\frac{L}{t}$	$\frac{d}{t}$	$\frac{D}{t}$	$\frac{W}{t}$	$\frac{\delta}{t}$	$\frac{F}{t^2E}$

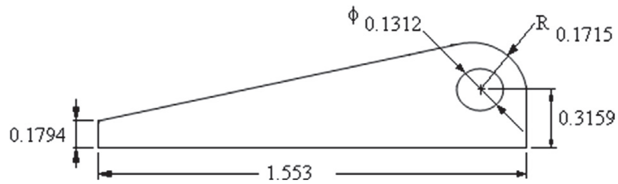

All dimensions are in m.

Figure 2 Prototype pad-eye dimensions.

The loads for the system will be the maximum design loads of the manufacturer. The dimensions of the pad-eye are given in Fig. 2:

$t = 0.1016$ m, F_{Max} = the load on the sling line = 1159 kN and $E = 210$ GN/m^2.

From Eq. (1) the relation will be

$$\sigma = S\frac{F \cdot D}{t^2 d} = (253.19) S \cdot F \tag{5}$$

By applying the same sequence to drive a relation between F and δ

$$\delta = K\frac{F \cdot D}{E \cdot t \cdot d} = (1.225 \times 10^{-10}) K \cdot F \tag{6}$$

4. Results and discussion

4.1. Deriving the equations factors for the prototype

Using Solid works a 3D model of the pad-eye is built and its material is specified as plain carbon steel. Then the welded face is selected. Also the force applied on the prototype is to be added with its direction. Finally the QOSMOSX is used to mesh the model with the default meshing method in the program and analyzing it to calculate the maximum stress and displacement of the model. Descending values for the applied force were used to calculate the maximum stress and displacement for the model. Then the average values for the applied forces with the resultants stresses and displacements are to be used in Eqs. (5) and (6) to calculate the stress and displacement factors S and K, the following step have been precede:

1. Building a 3D model for the prototype the pad-eye and specify its material.
2. Determine the welding face and adding the amount and direction of the maximum load.
3. Subdivide the pad-eye to meshing elements and then analyze the model to calculate and locate the maximum stress and displacement.

4.2. Mesh information

1. The analysis is to be run in order to determine the factor of safety.
2. The stress distribution results are to be checked to determine the maximum stress on the model.
3. The maximum displacement is to be checked.
4. By applying the same sequence from steps 1–6 with different values of F the values for S and K are derived and the results of the Stress σ and displacement δ are to be obtained from the software Solid works. Figs. 3 and 4 show the force versus maximum stress and maximum displacement of the prototype.

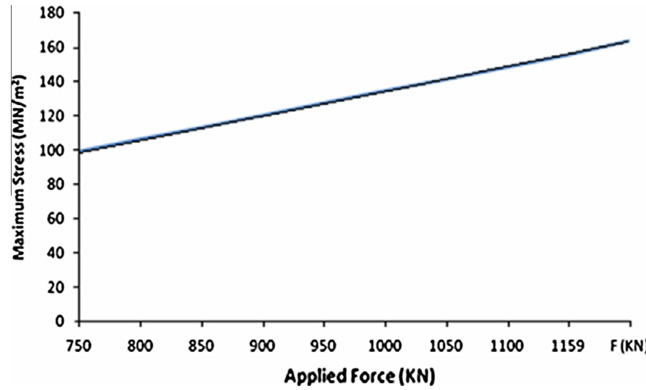

Figure 3 Force versus maximum stress for the prototype.

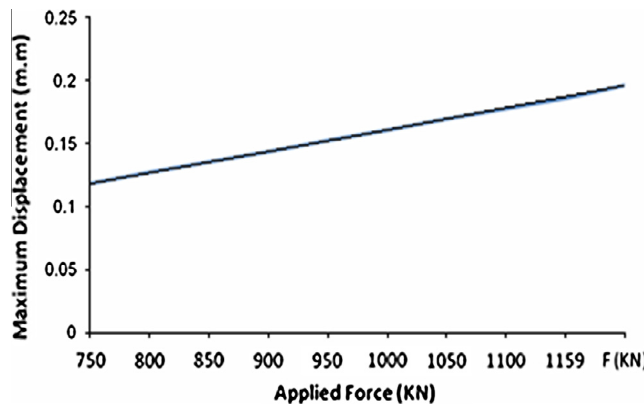

Figure 4 Force versus maximum displacement for the prototype.

The values for S_{pr} and K_{pr} become

$$S_{pr} = \frac{\Sigma\sigma}{(253.12)\Sigma F} \text{ and } K_{pr} = \frac{\Sigma\delta}{(1.225 \times 10^{-10})\Sigma F}$$

Hence $\Sigma\sigma = 13{,}095$ MN/m^2, $\Sigma\delta = 1.5698$ mm and $\Sigma F = 9259$ kN, then $S_{pr} = 0.559$ and $K_{pr} = 1.384$.

4.3. Deriving the equations factors

Similarity conditions require that the equations of two similar systems be the same. If the r-terms of the functional equation for two systems are the same, then $f_1 = f_2$ even if the functional equation is completely not known. These equalities of r-terms which determine the conditions, for which the two systems are similar, are the similarity conditions or scaling laws for these systems and for the specific phenomena.

$\pi_{1p} = f_p(\pi_{2p}, \pi_{3p}, \pi_{4p}, \ldots, \pi_{8p})$, $\pi_{1m} = f_m(\pi_{2m}, \pi_{3m}, \pi_{4m}, \ldots, \pi_{8m})$
If $\pi_{1p} = \pi_{1m}$ for $i = 2, 3, 4, \ldots, 8$, then
$f_p(\pi_{2p}, \pi_{3p}, \pi_{4p}, \ldots, \pi_{8p}) = f_m(\pi_{2m}, \pi_{3m}, \pi_{4m}, \ldots, \pi_{8m})$

Since these 1r-terms are combinations of geometric, dynamic, material, and kinematic parameters of the systems, the above equalities define different similarities, such as geometric , material, kinematic, and dynamic similarity [12].

4.4. Models scaling tests

The relations have been tested by calculating the S and K factors for the nine models by scaling all the system factors using the same scale factor λ.

- Model-1 $\lambda_1 = (0.9)$: the sequence for analysis the model is used as the prototype with considering the following:

1. The sketch and extrude dimensions will be scaled to 0.9 of the prototype dimensions as follows:
   $t_1 = \lambda_1 .\ t_P = 0.9\ (0.1016) = 0.09144$ m, $D_1 = \lambda_1 .\ D_P = 0.9\ (0.3429) = 0.30861$ m
   $d_1 = \lambda_1 .\ d_P = 0.9\ (0.1312) = 0.11808$ m
2. Same material is to be considered (plain carbon steel).
3. Using the same restraints.
4. Applying $F_1 = \lambda_1 .\ F_p = 0.9(1{,}159{,}000) = 1{,}043{,}100$ N on the same face and direction.
5. Show the predicted stress and displacement distribution for the model.

Theoretically in case of complete similarity that S_P equal to S_m, also K_p equal K_m. By substituting the model dimensions values into Eqs. (5) and (6) the theoretical values for the maximum stress and maximum displacement are calculated.

$$\sigma = S\frac{F \cdot D_1}{t_1^2 d_1} = (0.559)F\frac{0.30861}{(0.09144)^2(0.11808)}, \delta = K\frac{F \cdot D_1}{E \cdot t_1 \cdot d_1} = (1.384)F\frac{(0.30861)}{(2.1 \times 10^{11})(0.11808)(0.09144)}$$

6. The deviation percentage between the predicted and theoretical stress and displacement is also calculated from

$$\sigma_{\%Dev} = \frac{\sigma_{Pr.} - \sigma_{Tr.}}{\sigma_{Pr.}} \times 100 \text{ and } \delta_{\%Dev} = \frac{\delta_{Pr.} - \delta_{Tr.}}{\delta_{Pr.}} \times 100$$

Accordingly by applying the same steps on the eight other models the dimensions for all models are obtained. The relation between the applied force and the theoretical and predicted values of the maximum stress for the models is shown in Fig. 5. The relation between the applied force and theoretical and predicted values of the maximum displacement for the models is shown in Fig. 6. The maximum displacement predicted and theoretical values are shown in Figs. 7 and 8 respectively.

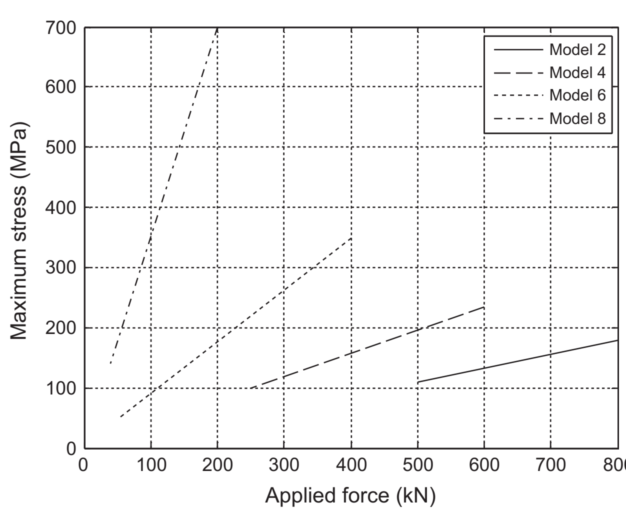

Figure 5 Predicted maximum stress for models 2, 4, 6, and 8.

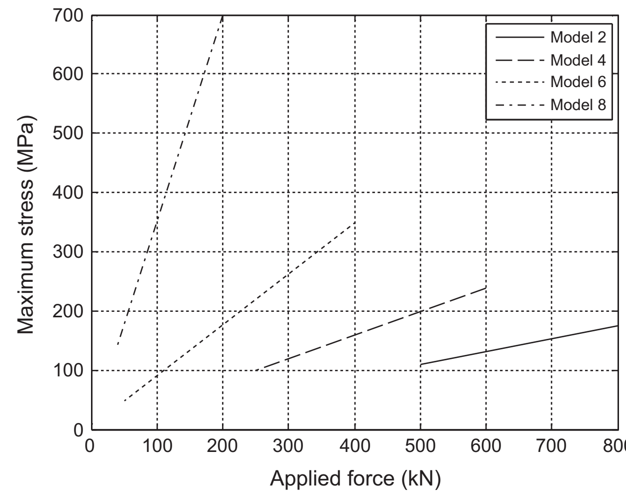

Figure 6 Theoretical maximum stress for models 2, 4, 6 and 8.

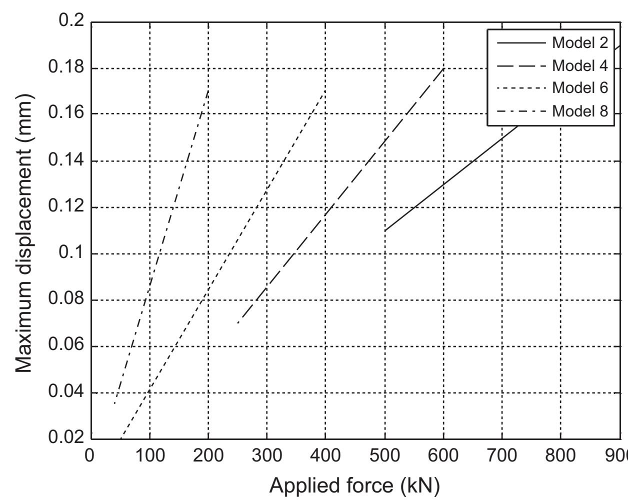

Figure 7 Predicted maximum displacement for models 2, 4, 6, and 8.

4.5. Discussion

By observing the charts of the stress and displacement for the selected models it seems that the deviations between the theoretical and predicted are very small to be noticed on the charts. So the average percentage deviation between the predicted and theoretical values for the maximum stress and maximum displacement for each model needs to be calculated in terms of the percentage deviation as

$$\%\text{Dev} = \frac{\text{Pr.} - \text{Th.}}{\text{Pr.}} \times 100.$$

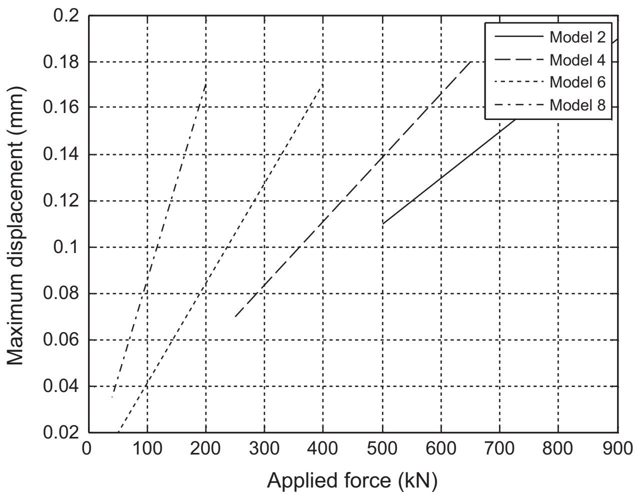

Figure 8 Theoretical maximum displacement for models 2, 4, 6, and 8.

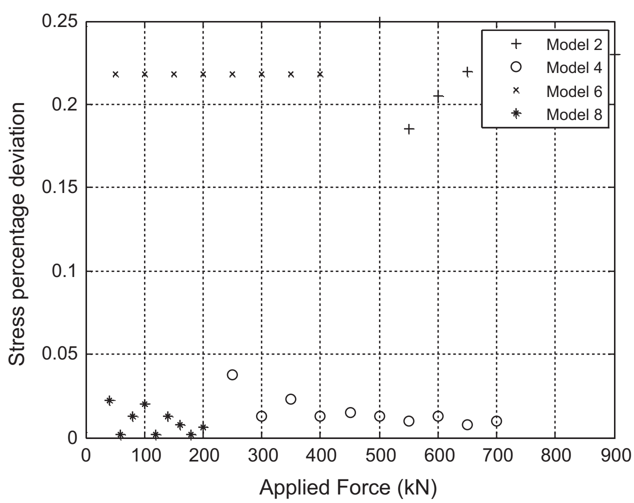

Figure 9 Percentage deviation of the theoretical to the predicted values of the maximum stress for the different models.

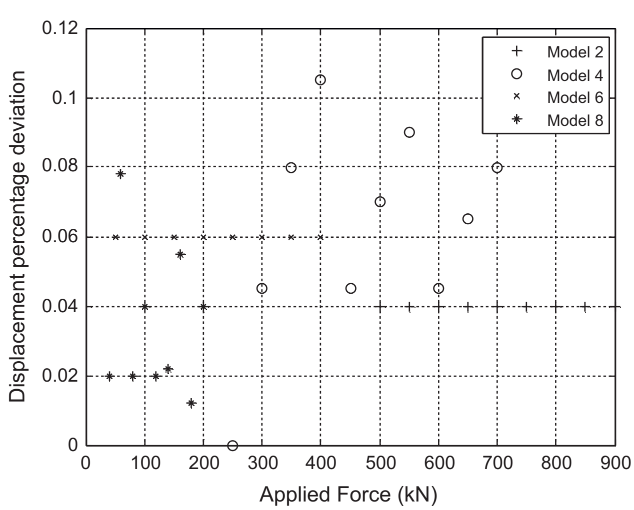

Figure 10 Percentage deviation of the theoretical to the Predicted values of the maximum displacement for the different models.

The percentage deviations for each model are calculated for the maximum stress and maximum displacement as shown in Figs. 9 and 10. It is clear that the percentage deviation whether for the maximum stress or for the maximum displacement does not exceed 0.25%.

5. Conclusions

- It is possible to use the dimensional analysis to derive equations to control the relations between the pad-eye characteristics and predict the values of the stress and displacement for any scaled model within the same materials by applying the scaling laws through Buckingham theorem.
- The percentage deviation in the results between the theoretical results and predicted values of the maximum stress and maximum displacement is quite small and does not exceed 0.25%.
- It has been shown here that the development of similitude relations for various homogeneous structural problems is a rather simple feasible task.
- The smallness of the deviation between the theoretical and the predicted results requires to be confirmed by experimental verification for structural elements of rather complicated shapes and for different loading applications and conditions.

References

[1] H. Chanson, Turbulent air–water flows in hydraulic structures: dynamic similarity and scale effects, Environ. Fluid Mech. 9 (2009) 125–142.

[2] C.S. Chouchaoui, P. Parks, O.O. Ochoa, Similitude study for a laminated cylindrical tube under tension, torsion, bending, internal and external pressure, Compos. Struct. 44 (1999) 231–236.

[3] M.E. Ephraim, O.T. Thom-Manuel, E.O. Rowland-Lato, Structural modeling of stability of plane sway frames, Int. J. Civ. Eng. Reas. 2 (2012) 4.

[4] X.Y. Gang, D.F. Wang, J.X. Su, A new similitude analysis method for a scale model test, Key Eng. Mater. 439–440 (2010) 704–709.

[5] V. Heller, Scale effects in physical hydraulics engineering models, JHR 49 (3) (2011) 293–306.

[6] P. Hertkorn, S. Rudolph, Dimensional analysis in case-based reasoning, in: Proceedings of the International Workshop on Similarity Methods, University of Stuttgart, Germany, 1998, pp. 163–178.

[7] S.J. Kline, Similitude and Approximation Theory, Springer, 2011.

[8] R. Letchworth, Space station: a focus for the development of structural dynamics scale model technology for large flexible space structures, in: Structural Dynamics and Materials Conference, Williamsburg, Virginia, April 21–22, 1988.

[9] P.F. Mendez, F. Ordonez, Scaling laws from statistical data and dimensional analysis, J. Appl. Mech. 72 (2005) 648–657.

[10] Y. Qian, S.R. Swanson, R.J. Nuismer, R.B. Bucinell, An experimental study of scaling rules for impact damage in fibre composites, J. Compos. Mater. 24 (1990) 559–570.

[11] M. Safoniuk, J.R. Grace, L. Hackman, C.A. Mcknight, Use of dimensional similitude for scale-up of hydrodynamics in three-phase fluidised beds, Chem. Eng. Sci. 54 (1999) 4961–4966.

[12] Kozo Saito, Progress in Scale Modeling, Springer, 2008.

[13] G.J. Simitses, J. Rezaeepazhand, Structural similitude for laminated structures, Compos. Eng. 3 (1993) 751–765.

[14] G.I. Simitses, J.H. Starnes, J. Pezaeepazhand, Structural Similitude and Scaling Laws for Plates and Shells, Springer, 2002.

[15] M. Taylor, I.A. Diaz, L.A.J. Sanchez, R.J.V. Mico, A matrix generalization of dimensional analysis: new similarity transforms to address the problem of uniqueness, Adv. Studies Theor. Phys. 2 (20) (2008) 979–995.

[16] Sh. Torkamani, H.M. Navazi, A.A. Jafari, M. Bagheri, Structural similitude in free vibration of orthogonally stiffened cylindrical shells, Thin-Walled Struct. 47 (2009) 1316–1330.

[17] D. Vassalos, Physical modeling and similitude of marine structures, Ocean Eng. 26 (1999) 111–123.

[18] G.A. Vignaux, J.L. Scott, Simplifying regression models using dimensional analysis, Aust. New Zealand J. Stat. 41 (1) (1999) 31–42.